# An 8 GHz high power AlGaN/GaN HEMT VCO*

Chen Huifang(陈慧芳)†, Wang Xiantai(王显泰), Chen Xiaojuan(陈晓娟),
Luo Weijun(罗卫军), and Liu Xinyu(刘新宇)

*(Key Laboratory of Microelectronics Device & Integrated Technology, Institute of Microelectronics, Chinese Academy of Sciences, Beijing 100029, China)*

**Abstract:** A high power X-band hybrid microwave integrated voltage controlled oscillator (VCO) based on AlGaN/GaN HEMT is presented. The oscillator design utilizes a common-gate negative resistance structure with open and short-circuit stub microstrip lines as the main resonator for a high $Q$ factor. The VCO operating at 20 V drain bias and –1.9 V gate bias exhibits an output power of 28 dBm at the center frequency of 8.15 GHz with an efficiency of 21%. Phase noise is estimated to be –85 dBc/Hz at 100 kHz offset and –128 dBc/Hz at 1 MHz offset. The tuning range is more than 50 MHz. The dominating effect of GaN HEMT's flicker noise on oscillator phase noise performance has also been discussed. The measured results show great promise for AlGaN/GaN HEMT technology to be used in high power and low phase noise microwave source applications.

**Key words:** AlGaN/GaN HEMT; negative resistance VCO; high power; phase noise; flicker noise
**DOI:** 10.1088/1674-4926/31/7/074012 **EEACC:** 1230B

## 1. Introduction

AlGaN/GaN high electron mobility transistor (HEMT), with its high breakdown voltage and high-frequency operation, is a promising device technology for high power applications at RF, microwave, and millimeter-wave frequency. Owing largely to the high electron sheet charge density, high saturation velocity, good thermal conductivity, and high electrical breakdown field, AlGaN/GaN HEMT-based devices are capable of delivering a significantly higher power with good efficiency for power amplifier applications than other semiconductor technologies. However, only a few results have been reported for microwave GaN HEMT-based VCOs.

At the microwave bands, the higher output power capability of GaN technology offers the advantage of generating high power levels directly from the VCO, eliminating the need for buffer amplifiers which consume additional DC power, increase noise, increase module complexity, and increase cost[1]. The reduction in system complexity is particularly useful for applications requiring very compact transceiver modules, such as mobile-phones, PDAs, and active phased arrays. The high power oscillators have been reported in Ref. [2] with 1.9 W of output power (DC-to-RF efficiency of 21.5%), in Ref. [3] with 1.7 W of output power, and in Ref. [4] with a DC-to-RF efficiency of 40.5%.

However, the higher flicker noise corner frequency of HEMTs compared to CMOS and HBT devices limits the HEMT oscillators' phase noise characteristics. Whereas, the AlGaN/GaN HEMT oscillators are also showing low phase noise reported in Ref. [5] with –118 dBc/Hz phase noise at 100 kHz offset and in Ref. [6] with –105 dBc/Hz phase noise at 100 kHz offset, which can compete against with its more mature counterparts. So if the improvement in noise continues as GaN technology becomes more mature, AlGaN/GaN HEMT will be an ideal choice for use in microwave source applications since using this technology can reduce overall system size, cost and complexity.

In this paper, we report on an 8 GHz GaN HEMT hybrid integrated VCO. The work adopts AlGaN/GaN HEMT technology independently researched and developed by the Institute of Microelectronics, CAS. The VCO with a 0.35 $\mu$m gate length and 1 mm total gate width (10 fingers) single HEMT exhibited a center frequency at 8.15 GHz with a tuning range of 50 MHz, high output power of 28 dBm at a supply $V_{\rm D} = 20$ V, $V_{\rm G} = -1.9$ V, $I_{\rm D} = 150$ mA, low phase noise of $-85$ dBc/Hz @ 100 kHz offset and $-128$ dBc/Hz @ 1 MHz offset. In addition, the measurement results showed that flicker noise corner frequency $f_{\rm c}$ of the GaN HEMT we used was approximately 700 kHz.

## 2. Oscillator configuration and design

This work is based on the GaN HEMT process of the Institute of Microelectronics, CAS. The device structure is shown in Fig. 1. The GaN HEMT was fabricated using a field-modulating plate (FP) and a recessed gate structure process[7]. An undoped AlGaN/GaN heterojunction FET was grown on a 4H SiC substrate. The gate length was chosen to be 0.35 $\mu$m, and the total gate width was 100 $\mu$m $\times$ 10 fingers. The device had characteristics of $I_{\rm max} = 0.85$ A/mm, $V_{\rm pinchoff} = -3$ V, and $g_{\rm m} = 313$ mS/mm. The current gain and power gain cut-off frequencies were about 28 and 38 GHz, respectively.

Oscillators can generally be categorized as either amplifiers with positive feedback satisfying the Barkhausen criteria[8], or as negative resistance circuits[9]. In most microwave oscillators, the negative resistance design technique is favored. It is shown in Fig. 2 where an oscillator circuit is separated into

* Project supported by the State Key Development Program for Basic Research of China (No. 2010CB327500) and the National Natural Science Foundation of China (No. 60890191).
† Corresponding author. Email: chenhf_128@yahoo.com.cn
Received 1 February 2010, revised manuscript received 12 March 2010 

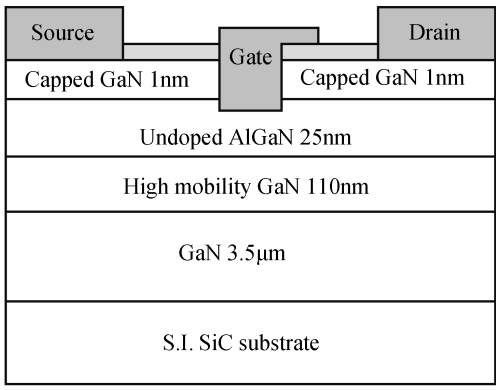


Fig. 1. AlGaN/GaN FP-HEMT structure.

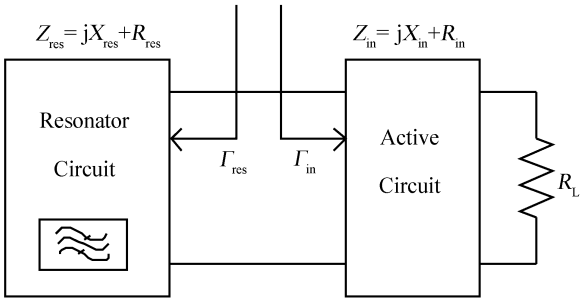


Fig. 2. A negative resistance oscillator model.

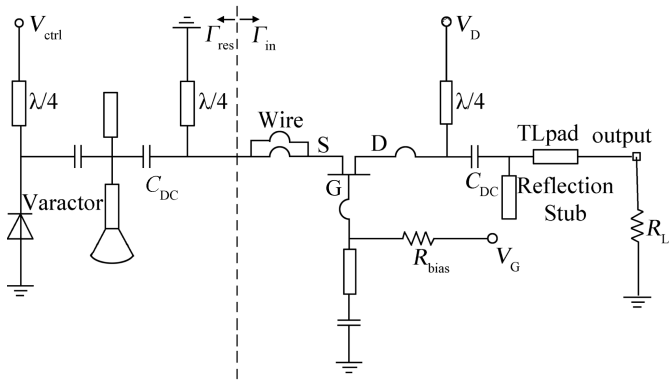


Fig. 3. AlGaN/GaN HEMT VCO schematic.

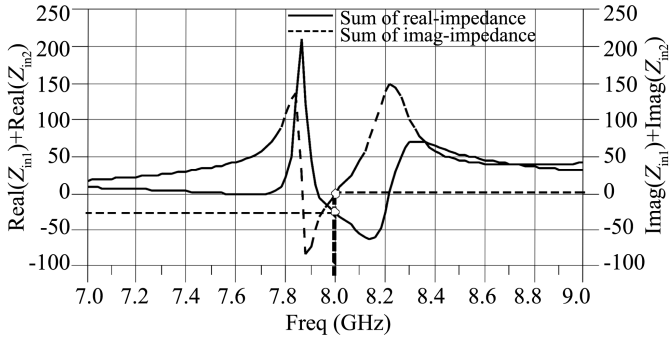


Fig. 4. Small-signal $S$-parameter simulations.

one-port passive components (typically including a resonator) and one-port active components that generate RF power. Assume that the active and the frequency-determining resonator circuits are modeled by two impedances $Z_{in} = jX_{in} + R_{in}$ and $Z_{res} = jX_{res} + R_{res}$, and that the reflection coefficients are $\Gamma_{in}$ and $\Gamma_{res}$ respectively.

Since only small-signal $S$-parameters are acquired by our own GaN HEMT process, the design will base on the following start-up oscillation conditions[9]:

$$X_{res} + X_{in} = 0, \quad R_{res} + R_{in} < 0, \tag{1}$$

or

$$|\Gamma_{in}\Gamma_{res}| > 1, \quad \phi_{in} + \phi_{res} = 0. \tag{2}$$

The design of the oscillator presented here adopts a common-gate AlGaN/GaN HEMT with 0.35 $\mu$m gate length and 1 mm total gate width. The measured small-signal $S$-parameter of the HEMT is used. The schematic circuit of the VCO is shown in Fig. 3. The HEMT device was connected in common-gate negative resistance configuration. Drain bias ($V_D = 20$ V) and varactor control voltage ($V_{ctrl} = 0-5$ V) were provided by $\lambda/4$ microstrip transmission lines. Gate electrode negative bias ($V_G = -1.9$ V) was supplied through a resistor. An inductive feedback connected to the HEMT's gate electrode in conjunction with the output matching network connected to the drain electrode were designed to make the active device unstable and maximize input negative resistance.

A high-$Q$ microstrip resonator composed of open-circuit stub in paralleled with short-circuit stub and radial stub was connected to the source electrode of the HEMT. As the lengths of microstrip lines changed, the slope of the resonator phase curve changed with it. A larger slope means a higher $Q$ factor. A varactor diode acted as a sub-resonator to control the phase of the resonator to vary the oscillation frequency. It was coupled to the main resonator through a chip capacitor. The varactor used here was an SMV1231 hyperabrupt junction varactor diode from Skyworks, which was designed for use in VCOs with low tuning voltage operation. When the resonator's capacitive impedance compensates with the HEMT's input inductive impedance, the start-up oscillation conditions [Eqs. (1) and (2)] are satisfied and the circuit oscillates.

The output was taken from the HEMT drain electrode. The open-circuit stub in the output matching network was used to improve the input reflection coefficient. A long series microstrip line TLpad connected the transistor drain to the circuit's RF output pad.

The architecture of the GaN HEMT used in the design was a square chip with six bond wire pads: a gate pad, a drain pad and four source pads. Bond wires were added to connect the transistor to the circuit. The bond wires created some inductance, which should be considered during simulation.

The VCO circuit was designed and simulated by Agilent advanced design system (ADS). Based on linear small-signal $S$-parameter analysis, simulated real and imaginary parts of the input and resonator impedances are shown in Fig. 4. Oscillation occurs at 8 GHz, at which the sum of input and resonator reactances is zero, while the sum of input and resonator resistances is less than zero.

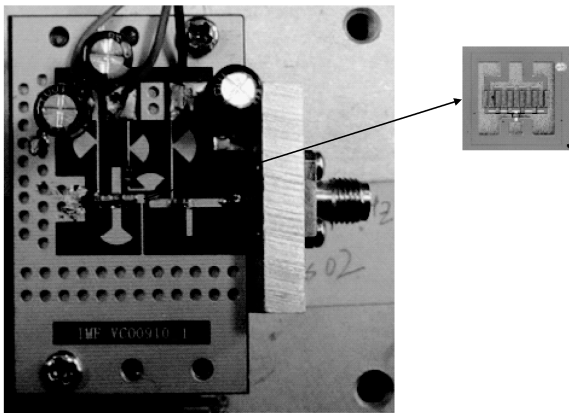

Fig. 5. Photograph of the VCO in test fixture.

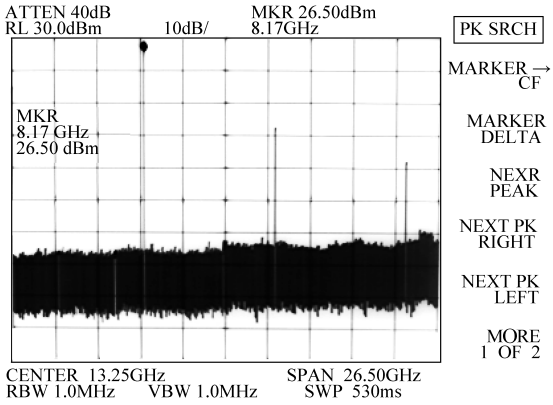


Fig. 6. Output spectrum of fundamental and harmonics.

## 3. Fabrication and test results

The hybrid integrated VCO was made on a Taconic PTFE printed circuit board (PCB) with dielectric constant = 2.55 and substrate thickness = 0.508 mm. The photograph of the VCO with a test fixture is shown in Fig. 5. The GaN device was mounted on the fixture in order to dissipate the heat generated by the high power device. Its three electrodes were connected to the circuit by bonding wires.

The VCO has been characterized in terms of oscillation frequency, output power, and phase noise by using an Agilent 8563E spectrum analyzer. Figure 6 shows output power and oscillation frequency measured with $V_{\rm D} = 20$ V, $V_{\rm G} = -1.9$ V, and $V_{\rm ctrl} = 1$ V. The oscillator delivered 26.5 dBm power at 8.15 GHz into 50 Ω load. Taking the insertion loss of the cable and test fixture into consideration, the output power was almost 28 dBm, with DC-to-RF efficiency of 21%. The second harmonic suppression was more than 25 dBc. When the control voltage tuned from 0 to 5 V, the VCO exhibited a tuning range of more than 50 MHz with average $K_{\rm vco}$ 10 MHz/V. Figures 7(a) and 7(b) shows phase noise measured at 100 kHz offset and 1 MHz offset respectively. The VCO demonstrated SSB phase noise of –85 dBc/Hz @ 100 kHz and –128 dBc/Hz @ 1 MHz. It has shown an obvious decrease in phase noise from 100 kHz to 1 MHz offset, which implied the dominating effect of the flicker noise of GaN HEMT.

Flicker noise is the primary contributor to the oscillator

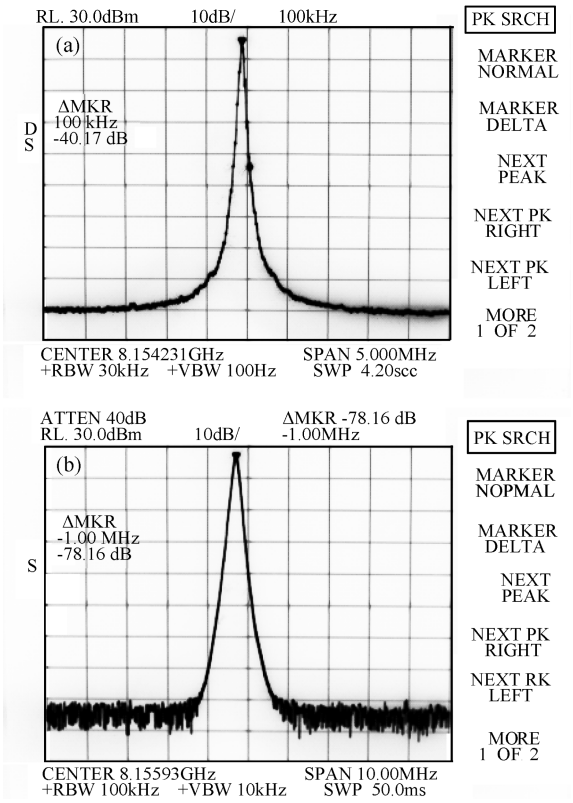


Fig. 7. Phase noise measurement versus the offset frequency. (a) At 100 kHz offset, RBW = 30 kHz. (b) At 1 MHz offset, RBW = 100 kHz.

phase noise spectrum at low offsets. Its power spectral density is proportional to $f^{-\gamma}$, where $\gamma$ is generally close to one but runs in a range depending on device types and bias condition[10, 11]. Leeson[12] has summarized the most significant causes of phase noise in oscillators:

$$L(f_{\rm m}) = 10\lg\left\{\frac{1}{2}\frac{kTF}{P_{\rm s}}\left(1+\frac{f_{\rm c}}{f_{\rm m}}\right)\left[1+\left(\frac{f_0}{2Q_{\rm L}f_{\rm m}}\right)^2\right]\right\} + 20\lg\frac{\sqrt{2}K_{\rm vco}\sqrt{4kTR_{\rm eq}}}{2f_{\rm m}}, \tag{3}$$

where $f_{\rm c}$ is flicker noise corner frequency of the device, and $Q_{\rm L}$ is the loaded quality factor. Figure 8 shows phase noise roll-off characteristics as a function of offset frequency. Since GaN HEMT has a higher corner frequency $f_{\rm c}$ than other mature semiconductor technologies, it exhibits phase noise performance as Fig. 8(a), $f_{\rm c} > \frac{f_0}{2Q_{\rm L}}$. The SSB phase noise has a slope of $f^{-2-\gamma}$ at offset frequencies below the resonator half-bandwidth $\frac{f_0}{2Q_{\rm L}}$, a slope of $f^{-\gamma}$ at offsets greater than $\frac{f_0}{2Q_{\rm L}}$ and less than $f_{\rm c}$. Above $f_{\rm c}$, the SSB phase noise floor is flat.

According to the above analysis, we can give a rough estimate of the corner frequency $f_{\rm c}$ of the GaN HEMT used here. As shown in Figs. 7(a) and 7(b), the slope of phase noise spectrum was high at low offset frequencies, and exponentially decreased across frequency. After a particular $f$, it is almost smooth. That $f$ is corner frequency $f_{\rm c}$. The phase noise spectrum changed first sharply then smoothly versus offset frequencies, indicating that the corner frequency was between 100 kHz

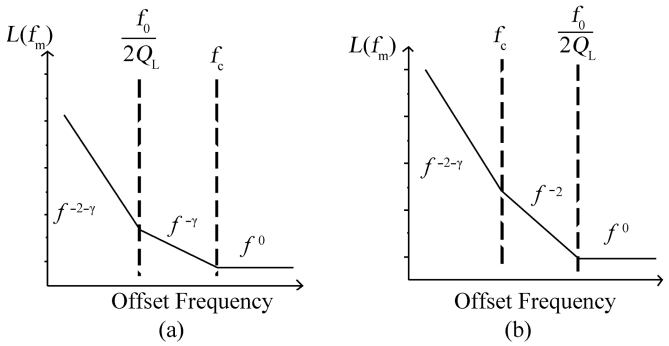


Fig. 8. Oscillator SSB phase noise characteristics. (a) $f_c > \frac{f_0}{2Q_L}$. (b) $f_c < \frac{f_0}{2Q_L}$.

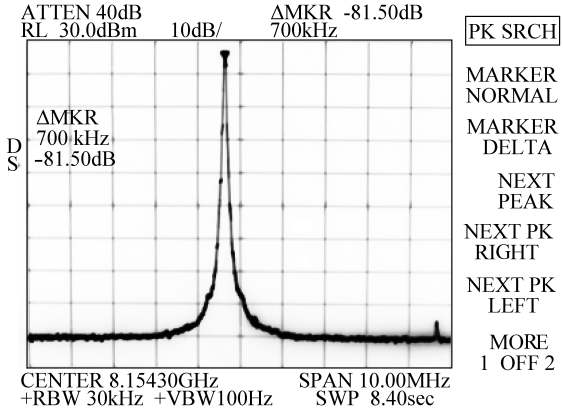


Fig. 9. Estimated flicker noise corner frequency.

and 1 MHz. Figure 9 shows that the GaN HEMT device we used has a corner frequency of approximately 700 kHz.

## 4. Conclusion

An 8 GHz high power hybrid integrated VCO has been demonstrated. The work is based on AlGaN/GaN HEMT technology independently developed by the Institute of Microelectronics. The VCO adopted a common-gate negative resistance structure with a high-$Q$ microstrip resonator. The measurement results showed an output power of 28 dBm at the center frequency of 8.15 GHz with a tuning range of more than 50 MHz. Phase noise was estimated to be –85 dBc/Hz at 100 kHz offset and –128 dBc/Hz at 1 MHz offset respectively. The flicker noise corner frequency was estimated to be 700 kHz. The dominating effect of flicker noise on the GaN HEMT-based oscillator phase noise performance has also been discussed.

From the above measurement results, we can conclude that the high voltage operation of GaN HEMT provides an excellent basis for the design of high output power oscillators. Besides, along with further improvement of AlGaN/GaN HEMT technology, especially the reduction of flicker noise and corner frequency, AlGaN/GaN HEMT-based oscillators will have an advanced performance on the phase noise levels. Excellent output power and low phase noise make AlGaN/GaN HEMT one of the most promising technologies for oscillator applications in very compact transceiver systems.

## References

[1] Shealy J, Smart J, Poulton M, et al. Gallium nitride (GaN) HEMT's: progress and potential for commercial applications. Gallium Arsenide Integrated Circuit (GaAs IC) Symposium, 2002: 243

[2] Xu H, Sanabria C, Heikman S, et al. High power GaN oscillators using field-plated HEMT structure. IEEE MTT-S International Microwave Symposium Digest, 2005: 1345

[3] Kaper V S, Tilak V, Kim H, et al. High-power monolithic AlGaN/GaN HEMT oscillator. IEEE J Solid-State Circuits, 2003, 38(9): 1457

[4] Kim J S, Wu W, Lin J, et al. High-efficiency GaN/AlGaN HEMT oscillator operating at L-band. APMC Microwave Conference, 2006

[5] Rice P, Sloan R, Moore M, et al. A 10 GHz dielectric resonator oscillator using GaN technology. IEEE MTT-S International Microwave Symposium Digest, 2004: 1497

[6] Vitusevich S A. Low-noise microwave devices: AlGaN/GaN high electron mobility transistors and oscillators. Physics and Engineering of Microwaves, Millimeter and Submillimeter Waves and Workshop on Terahertz Technologies, 2007

[7] Zheng Yingkui, Liu Guoguo, He Zhijing, et al. 0.25 $\mu$m gate-length AlGaN/GaN power HEMTs on sapphire with $f_T$ of 77 GHz. Chinese Journal of Semiconductors, 2006, 27(6): 963

[8] Jones M H. A practical introduction to electronic circuits. Cambridge University Press, 1982

[9] Vendelin G D. Design of amplifiers and oscillators by the $S$-parameter method. John Wiley & Sons Ltd, 1982

[10] Ho W, Suvaa C, Tong K Y. Study of $1/f$ noise in III–V nitride based MODFETs at low drain bias. Proceedings IEEE Electron Devices Meeting, 1999: 130

[11] Balandin A, Morozov S V, Cai S. Low flicker-noise GaN/AlGaN heterostructure field-effect transistors for microwave communications. IEEE Trans Microw Theory Tech, 1999, 47(8): 1413

[12] Leeson D B. A simple model of feedback oscillator noise spectrum. Proc IEEE, 1966, 54(2): 329